

Exact numerical study of the ground-state magnetic properties of clusters

F. López-Urías and G. M. Pastor

Laboratoire de Physique Quantique, Unité Mixte de Recherche 5626 du CNRS, Université Paul Sabatier, 118 route de Narbonne, F-31062 Toulouse, France

(Received 24 August 1998)

The ground states of bcc, fcc, hcp, and icosahedral clusters having $N=12-14$ atoms are calculated exactly in the framework of the Hubbard Hamiltonian by using Lanczos's numerical diagonalization method. The total spin S shows a diversity of remarkable, sometimes surprising behaviors as a function of Coulomb interaction strength U/t and band filling ν/N . The magnetic properties are analyzed, in particular, by relating them to the corresponding single-particle spectra. Changes of symmetry close to real-space shell closings at $N=13$ are discussed. The relative stability of the different cluster geometries is determined and the corresponding structural and magnetic diagrams are derived. Electron correlation effects close to half-band filling result in changes of structure that are often accompanied by important changes in the magnetic behavior. Ferromagnetism is found to be particularly stable for $\nu/N \approx 1.2-1.4$. The main trends as a function of N , ν and U/t are compared with previous exact diagonalization studies on smaller clusters. [S0163-1829(99)09907-5]

I. INTRODUCTION

Electron correlation in finite systems and the associated many-body phenomena, which distinguish small clusters from atoms and solids, are subjects of main interest in current cluster research. One of the most intensively studied, yet still challenging problems is magnetism. Transition metals (TM's), which in the bulk show itinerant d -electron magnetism, have motivated a large body of experimental and theoretical work.^{1,2} Stern-Gerlach (SG) deflection experiments on size-selected cluster beams have shown that Fe, Co, and Ni clusters are magnetic and that the low-temperature magnetic moments per atom are larger than the corresponding bulk magnetizations.¹ Even Rh, which is not magnetic in the solid state, presents significantly large magnetic moments if the size of the cluster is smaller than about 50 atoms. From SG measurements the temperature dependence of the average magnetization per atom has been also inferred.¹ Electronic structure calculations on TM clusters are performed by using mainly local-spin-density (LSD) or self-consistent tight-binding theories.² These have been quite successful in accounting for and sometimes even in predicting the low-temperature magnetic moments observed in experiment. However, in spite of their success, these types of calculations are intrinsically limited by the mean-field treatment of electron-electron interactions implied by the LSD or unrestricted Hartree-Fock approximations. A more profound understanding of the electronic correlations underlying the magnetic properties of clusters is not only important from a fundamental point of view but it is also likely to be crucial in investigations of more delicate properties such as the excitation spectra or the magnetic behavior at finite temperatures.

An accurate treatment of electron correlations poses a serious difficulty. Therefore, full many-body studies of the magnetic properties of clusters have only been achieved in the framework of simple models such as the single-band Hubbard model.³ Falicov and Victora⁴ studied a four-site tetrahedral cluster. They obtained the many-body eigenstates analytically with the aid of group theory and classified the

occurrence of magnetic ground states by means of Hund's rule applied to the cluster as if it were a single "structured atom." Ishii and Sugano⁵ considered three four-site systems, namely, the tetrahedron, the square, and the rhombus. They investigated the effects of electron correlations on the charge distribution of low-symmetry clusters, and determined the ground-state spin S and the relative stability of different structures for a few values of U/t . Callaway, Chen, and Tang⁶ extended the work of Ishii and Sugano in several respects. In addition to the four-site clusters considered in Ref. 5, four five-site clusters (pentagon, truss, square pyramid, and bipyramid) were studied. The ground-state spin S was determined as a function of U/t and ν , and the dependence of S on cluster geometry was related to the corresponding single-particle spectra. The energies of these structures were compared and several structural changes were identified, some of them triggered by magnetism. More recently, a systematic study of magnetism and structure of clusters within the Hubbard model has been reported for $N \leq 8$ atoms.⁷ In this case, the electron correlation problem was solved exactly by means of Lanczos numerical diagonalization method and at the same time a full geometry optimization was performed. All nonequivalent cluster topologies were considered in a similar way as in the tight-binding (Hückel) investigations of simple metals by Wang *et al.*⁸ While rigorous results concerning the interplay of electron correlations, magnetism, and cluster structure are available for $N \leq 8$, the properties of larger clusters remain for the most part unexplored.⁹

The purpose of this work is to determine the size and structural dependence of the magnetic properties of clusters having $N=12-14$ atoms by using the single-band Hubbard Hamiltonian and by considering a few representative structures. Electron correlations are treated exactly within a full many-body scheme. The considered size range is particularly interesting since a central atom with its 12 nearest neighbors (NN's) corresponds to a closed atomic shell in compact structures (e.g., fcc, hcp, or icosahedral clusters). Thus, one can study the role of real-space shell closings and of the

associated changes of symmetry on the magnetic behavior. Varying the cluster size around $N=13$ for a given type of structure and changing the cluster symmetry for a given size yield complementary information. The present calculations for sizes up to $N=14$ atoms are a significant extension with respect to available results for $N \leq 8$. They allow to gain further insight into the size dependence of the magnetic properties including correlation effects and should also be of interest in view of the properties of the Hubbard model in three-dimensional lattices. However, the simplicity of the Hamiltonian, in particular the assumption of a single orbital per atomic site, and the lack of unconstrained geometry optimizations precludes a detailed quantitative comparison with the experimental results on ferromagnetic TM clusters.¹

The outline of the paper is the following. In Sec. II we briefly recall the model and method of calculation. Our results are presented and discussed in Sec. III. First, the ground-state spin S of icosahedral, fcc, hcp, and bcc clusters is determined as a function of band filling ν/N and Coulomb repulsion strength U/t . Trends for different geometries are compared and the structural dependence of the magnetic properties is analyzed. Then, the relative stability of the considered structures is obtained by comparing the ground-state energies. Structural and magnetic transitions are identified. Finally, Sec. IV summarizes our conclusions.

II. MODEL AND METHOD OF CALCULATION

In order to calculate the electronic and magnetic properties of the clusters, we consider the Hubbard Hamiltonian³

$$H = -t \sum_{\langle i,j \rangle, \sigma} \hat{c}_{i\sigma}^\dagger \hat{c}_{j\sigma} + U \sum_i \hat{n}_{i\uparrow} \hat{n}_{i\downarrow}. \quad (2.1)$$

As usual, $\hat{c}_{i\sigma}^\dagger (\hat{c}_{i\sigma})$ refers to the creation (annihilation) operator for an electron at site i with spin σ , and $\hat{n}_{i\sigma} = \hat{c}_{i\sigma}^\dagger \hat{c}_{i\sigma}$ is the corresponding number operator. The first term is the kinetic-energy operator, which describes electronic hopping between NN sites i and j leading to electron delocalization and bond formation ($t > 0$). The second term takes into account the intra-atomic Coulomb repulsion, which is the dominant contribution from the electron-electron interaction ($U \geq 0$).³ The dynamics of the valence electrons results from the interplay of these two simple terms and their relative importance can be characterized by the dimensionless parameter U/t . The electronic properties are the result of a delicate balance between kinetic and Coulomb energies, which depends on U/t and on the total spin S . In addition, the ground state corresponding to different cluster structures may be of very different nature.⁴⁻⁷ Therefore, the determination of the magnetic and structural behavior of clusters requires an accurate treatment of electron correlations.

The Hubbard model is solved numerically by expanding its eigenfunctions $|\Psi_l\rangle$ in a complete set of basis states $|\Phi_m\rangle$, which have definite occupation numbers $n_{i\sigma}^m$ at all orbitals $i\sigma$, i.e., $\hat{n}_{i\sigma}|\Phi_m\rangle = n_{i\sigma}^m|\Phi_m\rangle$ with $n_{i\sigma}^m = 0$ or 1. $|\Psi_l\rangle$ is written as

$$|\Psi_l\rangle = \sum_m \alpha_{lm} |\Phi_m\rangle, \quad (2.2)$$

where

$$|\Phi_m\rangle = \left[\prod_{i\sigma} (\hat{c}_{i\sigma}^\dagger)^{n_{i\sigma}^m} \right] |vac\rangle. \quad (2.3)$$

The values of $n_{i\sigma}^m$ satisfy the usual conservation of the number of electrons $\nu = \nu_\uparrow + \nu_\downarrow$ and of the z component of the total spin $S_z = (\nu_\uparrow - \nu_\downarrow)/2$, where $\nu_\sigma = \sum_i n_{i\sigma}^m$. Taking into account all possible electronic configurations may imply a considerable numerical effort, which in practice sets a drastic limit to the size of the clusters under study. For example, at half-band filling and minimal S_z the dimension of the Hilbert space $D = \binom{N}{\nu_\uparrow} \binom{N}{\nu_\downarrow}$ is $D = 853\,776$, $2\,944\,656$, and $11\,778\,624$, for $N = 12$, 13 , and 14 , respectively. For not too large clusters, the expansion coefficients α_{lm} corresponding to the ground state ($l=0$) and low-lying excited states can be determined by sparse-matrix diagonalization procedures. In the present work we use a Lanczos iterative method.¹⁰ The ground state $|\Psi_0\rangle$ is calculated in the subspace of minimal S_z since this ensures that there are no *a priori* restrictions on S . The actual S is obtained by applying the operator

$$\hat{S}^2 = \sum_{ij} \mathbf{S}_i \cdot \mathbf{S}_j = \sum_{ij} \left[\frac{1}{2} (\hat{S}_i^+ \hat{S}_j^- + \hat{S}_i^- \hat{S}_j^+) + \hat{S}_i^z \hat{S}_j^z \right], \quad (2.4)$$

where $\hat{S}_i^+ = \hat{c}_{i\uparrow}^\dagger \hat{c}_{i\downarrow}$, $\hat{S}_i^- = \hat{c}_{i\downarrow}^\dagger \hat{c}_{i\uparrow}$, and $\hat{S}_i^z = (\hat{n}_{i\uparrow} - \hat{n}_{i\downarrow})/2$. The lowest excited states of different S are obtained by using an appropriate projector and by giving the desired spin symmetry to the starting vector $|0\rangle$ of the Lanczos procedure. In practice, we generate a random $|\tilde{0}\rangle$, just as for the ground-state calculation, and we project out one or more unwilled components of spin S' by the operation

$$|0\rangle = [\hat{S}^2 - S'(S'+1)]|\tilde{0}\rangle. \quad (2.5)$$

Alternatively, when the ground-state spin S_0 is low, one may obtain excited states of higher spin more easily by performing the calculations in subspaces of $S_z > S_0$.

Several cluster properties can be calculated in terms of the coefficients α_{lm} of the eigenstate $|\Psi_l\rangle$ by simple operations on the basis states $|\Phi_m\rangle$. For example, the spin-density distribution is given by

$$\langle \hat{n}_{i\sigma} \rangle_l = \sum_m |\alpha_{lm}|^2 n_{i\sigma}^m, \quad (2.6)$$

density-density correlation functions are obtained from

$$\langle \hat{n}_{i\sigma} \hat{n}_{j\sigma'} \rangle_l = \sum_m |\alpha_{lm}|^2 n_{i\sigma}^m n_{j\sigma'}^m, \quad (2.7)$$

and spin-correlation functions are given by

$$\langle \hat{S}_i^z \hat{S}_j^z \rangle_l = \frac{1}{4} \sum_m |\alpha_{lm}|^2 (n_{i\uparrow}^m - n_{i\downarrow}^m) (n_{j\uparrow}^m - n_{j\downarrow}^m). \quad (2.8)$$

Within a controlled accuracy, the results are exact in the framework of the model Hamiltonian H .

III. RESULTS AND DISCUSSION

In the following we present and discuss results on the magnetic properties of clusters having $N = 12-14$ atoms,

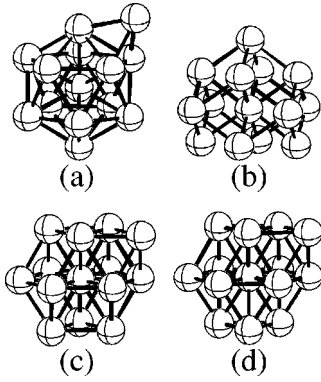


FIG. 1. Illustration of the structures considered for $N=14$ atoms: (a) icosahedral, (b) bcc, (c) fcc and (d) hcp clusters. For $N=13$ and $N=12$ one or two of the outermost atoms are removed.

which were obtained using the Hubbard Hamiltonian and exact diagonalization methods. Four different symmetries are considered: icosahedral clusters, that maximize the average coordination number; face-centered-cubic (fcc) and hexagonal-close-packed (hcp) clusters, as examples of compact structures that are found in the solid state; and body-centered-cubic (bcc) clusters, as an example of a rather open bipartite structure.¹¹ These cluster geometries, which are illustrated in Fig. 1, are representative of various types of structures found to be the most stable in rigorous geometry optimizations for $N \leq 8$.⁷ In Secs. III A–III C the magnetic behaviors of the different cluster geometries are analyzed. The electronic and magnetic properties are compared in Sec. III D. The relative stability between these structures is determined and the resulting magnetic transitions are discussed.

A. Icosahedral clusters

In Fig. 2 the ground-state spin S of icosahedral clusters is shown as a function of band filling ν/N ($2 \leq \nu \leq 2N-2$) for a few representative values of the Coulomb repulsion strength U/t . If Coulomb interactions are weak, for example for $U/t=1/8$, S is small and in most cases minimal (i.e., $S=0$ or $1/2$). This behavior is certainly expected since in the uncorrelated limit ($U=0$) equal filling of spin-up and spin-down single-particle (SP) states always yields the lowest energy. Only in the presence of a degenerate highest occupied SP level one may obtain that a magnetic state ($S \geq 1$) can be degenerate with the minimal-spin state for $U=0$. Of course, a nonvanishing Coulomb interaction (even if very small) may stabilize the $S \geq 1$ state and lead to a nondegenerate magnetic ground state. This is, in fact, the case for the icosahedron with $N=13$ atoms and $\nu=4-6$ electrons, since in this case a threefold degenerate level is partially filled (see Fig. 3). For $\nu=4$ there are two electrons in the degenerate manifold. Thus $S=1$ corresponds to a full spin polarization of these levels. The same holds for $\nu=5$ and $\nu=6$ yielding $S=3/2$ and $S=1$, respectively. Note that there are no spin polarizations beyond these threefold degenerate states, since this would imply a too large increase of the kinetic energy given by the promotion energy from the occupied minority spin to the unoccupied majority-spin levels. If an atom is removed or added to the perfect icosahedron, the symmetry of the cluster lowers and the threefold degenerate level splits.

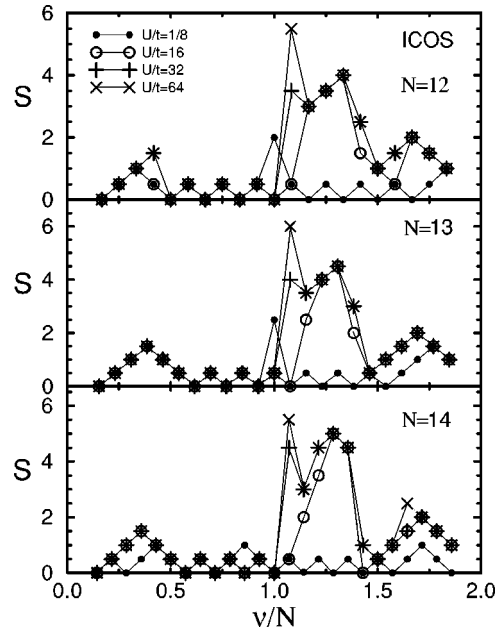


FIG. 2. Ground-state spin S of icosahedral clusters having $N=12-14$ atoms as a function of band filling ν/N . Representative values of U/t are considered as indicated in the inset. The lines connect points corresponding to the same U/t and are just a guide to the eye.

For $N=12$, this leaves two degenerate states that have a lower energy than the nondegenerate one (see Fig. 3). Therefore, as shown in Fig. 2 for $N=12$, $\nu=4$ continues to yield a magnetic state for $U/t=1/8$ ($S=1$), while $\nu=5$ and 6 show now minimal S . For $N=14$, the first threefold degenerate level of the 13-atom icosahedron splits in a nondegenerate level followed by two degenerate ones. Consequently, the trend is inverted. For $\nu=4$ and 5 , the ground state lowers its spin at small U/t , but $\nu=6$ remains magnetic ($N=14$).

The splitting of degeneracies and the resulting reduction of S for small U/t often become unimportant as the Coulomb interaction increases. Indeed, the clusters with $N=12$ and $N=14$ atoms recover a magnetic ground state just as in the perfect icosahedron provided that U/t is sufficiently large. For example, for $N=14$ and $\nu=4$ ($\nu=5$), $S=1$ ($S=3/2$) if $U/t \geq 11.7$ ($U/t \geq 5.6$). In contrast, for $N=12$ and $\nu=6$, the total spin $S=0$ for all U/t (even for $U/t \rightarrow +\infty$). Note that these differences occur despite the fact that the gap between highest occupied and lowest unoccupied SP levels

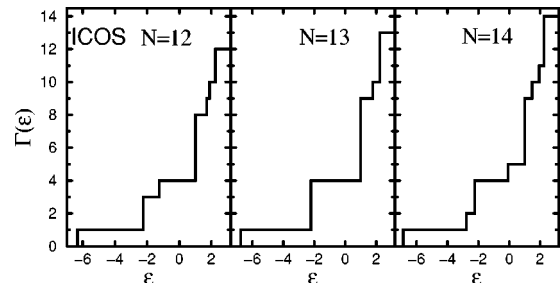


FIG. 3. Single-particle (SP) electronic structure of icosahedral clusters having $N=12-14$ atoms [$U=0$ in Eq. (2.1)]. The integral of the SP density of states per spin is shown: $\Gamma(\epsilon) = \sum_k \theta(\epsilon - \epsilon_k)$, where ϵ_k refers to the SP eigenvalues.

are of the same order of magnitude ($\varepsilon_4 - \varepsilon_3 = 0.99t$ for $N = 12$ and $\varepsilon_3 - \varepsilon_2 = 0.53t$ for $N = 14$). Similar relations between cluster symmetry, SP electronic structure and magnetic behavior in the weak-interacting regime are also found for other cluster structures and band fillings. However, simple trends are far from being a general rule. In some cases, an increase of the Coulomb interactions does not lead to an increase of S even if SP degeneracies are present at the Fermi energy. Examples of such many-body effects are discussed below.

Magnetic ground states at small Coulomb repulsions are also found when the number of electrons per atom is large, i.e., for a small number of holes $\nu_h = 2N - \nu$. As in the case of low-electron concentrations, the SP electronic structure is a useful starting point for discussing the band-filling dependence of the magnetic behavior. Here it is more convenient to analyze the results in terms of hole occupations.¹² For the symmetric icosahedron ($N = 13$) the highest antibonding state is threefold degenerate (see Fig. 3). It is therefore understandable that $S = \nu_h/2$ for $\nu_h \leq 3$ and $S = 3 - \nu_h/2$ for $3 \leq \nu_h \leq 6$ already at small U/t (e.g., $U/t = 1/8$). This corresponds to a saturated ferromagnetic state *within the threefold degenerate level*. Note that for small U/t there is no spin polarization beyond these degenerate states. The SP excitation energy is $\varepsilon_{11} - \varepsilon_{10} = 0.46t$.

The highest antibonding SP manifold splits in two after adding or removing an atom. For $N = 12$, a doubly degenerate level lies above a nondegenerate one (see Fig. 3). Thus, $S = 1$ for $\nu_h = 2$ and $S = 1/2$ or 0 for $\nu_h = 3$ and 4 . In contrast, for $N = 14$ the degeneracies are inverted resulting in a minimal S for $\nu_h = 2$ and 3 , while $S = 1$ for $\nu_h = 4$. As in the case of low electron concentrations ($\nu/N < 0.5$), the cluster symmetry plays a central role in determining the magnetic behavior in the limit of small U/t . However, the effect of small SP degeneracies is washed away by electronic correlations as the Coulomb interaction increases. Symmetry breaking around the perfect icosahedron loses importance at larger U/t and the band-filling dependence of S of all $N = 12-14$ icosahedra resemble each other. For example, for $U/t \geq 16$ the less symmetric 12- and 14-atom clusters also present saturated magnetism for $\nu_h \leq 3$. Moreover, small gaps in the SP spectrum are no longer an impediment to the development of large-spin polarizations. For $U/t = 16$ a maximum in S is found for $\nu_h = 4$ ($N = 12-14$) as if the highest four levels would belong to the same manifold (see Figs. 2 and 3). For $N = 14$ even a fifth state can be fully polarized provided that U/t is sufficiently large ($S = 5/2$ for $\nu_h = 5$ and $U/t \geq 56$). Incidentally, this fifth level of the $N = 14$ cluster (counted from above) can be regarded as coming from the splitting of a lower-lying fivefold degenerate level of the perfect icosahedron. Therefore, in this case symmetry lowering seems to favor the formation of a larger magnetic moment by approaching SP levels that were otherwise too far apart.

The previous discussion shows that at low carrier concentrations (ν or $\nu_h < 0.5$) the magnetic behavior of icosahedral clusters can be qualitatively understood as the result of filling successively a group of degenerate or nearly degenerate SP levels with maximal-spin polarization. This leads to maxima in S as a function of ν/N when the group of levels is half-filled, very much as if one would apply Hund's first rule for atomic shells to the degenerate (or nearly degenerate) mani-

folds found at the extremes of the SP electronic spectrum of the cluster. Remarkably, this physical picture holds even in the limit of very large Coulomb interaction.¹³ Two main reasons contribute to the validity of this simple interpretation: the presence of a well-defined group of levels having almost the same energy and the fact that the carrier concentration is low.

Close to half-band filling much more complex magnetic properties are observed. For small U/t (e.g., $U/t = 1/8$) the ground-state spin is minimal for almost all numbers of electrons (see Fig. 2 for $|\nu/N - 1| < 0.5$). Notice that low-spin states dominate in spite of the presence of important orbital degeneracies in the SP spectrum. For example, as shown in Fig. 3, a fivefold degenerate level is partially filled at $U = 0$ for $N = 13$ and $9 \leq \nu \leq 18$. Fourfold degeneracies are found for $N = 12$ and $N = 14$. This behavior contrasts with the previously discussed low-carrier-density limit ($\nu/N < 0.5$ and $\nu/N > 1.5$). Only in a few cases we obtain magnetic states at small U/t . These are, namely, $N = \nu = 12$ [$S = (12 - 8)/2$], $N = \nu = 13$ [$S = (13 - 8)/2$], and $N = 14$ with $\nu = 12$ [$S = (12 - 10)/2$]. They correspond to a full polarization of the electrons occupying the partially filled degenerate SP level and can be thus interpreted in a similar way as the magnetic states found for low carrier concentrations.

For small U the magnetic behavior below and above half-band filling are qualitatively similar ($1/2 < \nu/N < 3/2$). However, they become completely different as U/t increases. For $1/2 \leq \nu/N \leq 1$ the lowest possible S is obtained. Increasing U/t not only leaves S unchanged when it was already minimal, but it also reduces S in cases where SP degeneracies resulted in unsaturated $S \geq 1$ for small U (e.g., $N = \nu = 13$ or $N = \nu = 12$). There is no sign of ferromagnetism, even at very large U . Instead, antiferromagnetic NN spin correlations are observed.^{14,15} Only on two occasions ($\nu = 10$ for $N = 12$ and $N = 13$) S increases slightly to $S = 1$ in the limit of $U/t = \infty$.¹³ In any case, the fact that the ground-state spin is minimal or very small at large U/t reflects the crucial importance of electronic correlations that stabilize low-spin states with respect to ferromagnetic ones. Should the Hartree-Fock approximation be used, a ferromagnetic state would always be more stable for sufficiently large U/t .

Above half-band filling, ferromagnetism develops with increasing Coulomb repulsion ($1 < \nu/N < 3/2$). The U/t dependence of S is given in Fig. 4 for representative values of ν . In most cases S increases with U/t as one would expect from mean-field Hartree-Fock arguments (Stoner criterion). A remarkable exception is found for $N = 12$ with $\nu = 13$. Here we first observe that S increases from $S = 1/2$ to $S = 5/2$ at $U/t = 2.7$. This ferromagnetic state at small U can be interpreted as the polarization of electrons occupying a degenerate partially filled SP level [$S = (13 - 8)/2 = 5/2$, see Fig. 3]. Nevertheless, at larger U ($U/t > 4.5$) antiferromagnetic correlations dominate. S decreases back to $S = 1/2$ until for even larger U ($U/t = 17.9$) a new ferromagnetic state develops leading progressively to the fully polarized Nagaoka state. Saturated ferromagnetism is obtained in all cases for $\nu = N + 1$ and large U/t , in agreement with Nagaoka's theorem.¹⁶ Note, however, that the Coulomb repulsion corresponding to the onset of magnetism ($S \geq 1$) and to the fully polarized state [$S = (N - 1)/2$] are both much larger than in

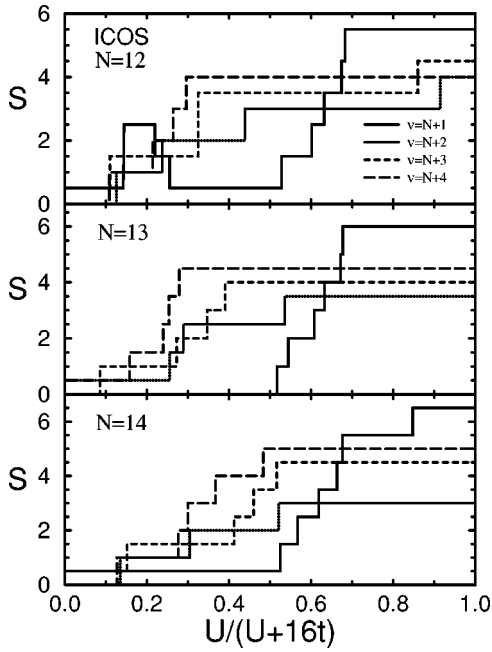


FIG. 4. Ground-state spin S of icosahedral clusters having $N = 12$ – 14 atoms as a function of the Coulomb interaction strength U/t . The numbers of electrons ν are indicated.

smaller clusters.⁷ For example, for $N=7$ ($\nu=8$, pentagonal bipyramid) $S=1$ for $U/t > 3.1$ and $S=3$ for $U/t > 16.4$, while for $N=13$ ($\nu=14$, icosahedron) $S=1$ for $U/t > 17.2$ and $S=6$ for $U/t > 33.6$. This is a consequence of the increasing importance of antiferromagnetic correlations as half-band filling is approached ($\nu/N = 1 + 1/N$).⁷ In fact, in the thermodynamic limit ($N \rightarrow \infty$) $\nu = N + 1$ presents a saturated ferromagnetic ground state only if $U/t = \infty$.

All the studied icosahedral clusters show that ferromagnetism is particularly stable at band fillings close to $\nu/N = 4/3$ ($\nu/N = 1.29$ – 1.36). For these ν/N ferromagnetism sets in at much smaller values of U/t than for Nagaoka's case ($\nu = N + 1$). Already $U/t = 16$ yields a saturated ferromagnetic ground state for $\nu = 16$ ($N = 12$), $\nu = 17$ ($N = 13$), and $\nu = 18$ or 19 ($N = 14$). Moreover, S presents here a maximum as a function of ν/N (see Fig. 2). This behavior, which is also observed for other cluster structures, may be interpreted as the result of two competing effects. On the one side, as ν/N is increased beyond $\nu/N = 1$ we move away from half-band filling where antiferromagnetism dominates. In particular, saturated ferromagnetism becomes more stable as more bonding minority-spin states are occupied ($\nu > N$). On the other side, as the number of electrons increases further, the carrier (hole) density becomes low enough so that the effects of Coulomb interactions are reduced very efficiently by correlations. Consequently, low-spin states dominate again for $\nu/N \approx 1.5$.

B. fcc and hcp clusters

The fcc and hcp clusters have close-packed structures with the same local coordination numbers but different point-group symmetries (Fig. 1). Their magnetic behavior shows many qualitative features in common, some of which are also shared by other compact structures such as the ico-

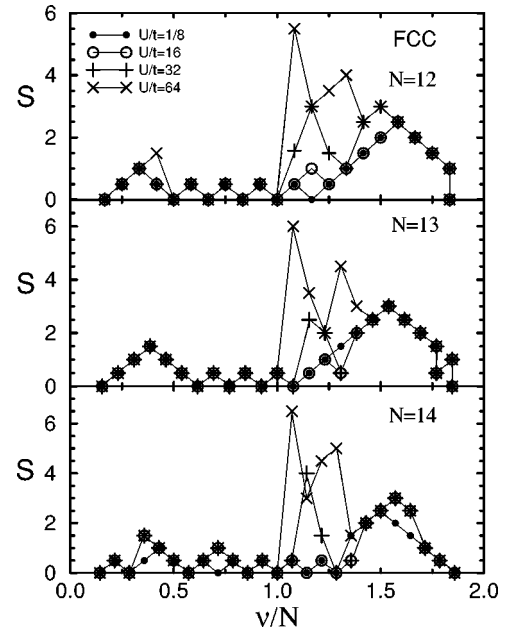


FIG. 5. Ground-state spin S of face-centered-cubic clusters having $N = 12$ – 14 atoms as a function of band filling ν/N . The Coulomb repulsions U/t are indicated. In some cases ($N = 12$ with $\nu = 22$ and $N = 13$ with $\nu = 23$ and 24) two values of S are given for the same U/t , which indicates a ground-state degeneracy.

hedron. However, the differences in symmetry and electronic structure result in specific magnetic properties as a function of N , ν , and U/t . The band-filling dependence of the ground-state spin of fcc clusters having $N = 12$ – 14 atoms is shown in Fig. 5. The corresponding SP spectra are given in Fig. 6. Results for hcp clusters are reported in Figs. 7 and 8. As already discussed in the previous section, magnetic states ($S \geq 1$) are obtained at low electron or hole concentrations ($\nu/N \leq 0.5$ and $\nu/N \geq 1.5$) even if U/t is very small (e.g., $U/t = 1/8$). This occurs whenever degeneracies are present in the SP electronic structure. In these cases (low carrier concentrations) S can be derived by applying Hund's first rule to the spectra shown in Figs. 6 and 8, as if the cluster would be a single structured atom.⁴ Consequently, maxima are obtained as a function of ν when a degenerate SP level is half-filled. Here, S corresponds to the full spin polarization of the highest occupied level and amounts to one-half the multiplicity of the highest occupied eigenvalue. For example, in the $N = 13$ fcc cluster, $S = 3/2$ for $\nu = 5$ and $S = 3$ for $\nu = 20$. The position of the maxima shift to $\nu = 4$ ($\nu = 6$) and $\nu = 19$ ($\nu = 21$) for $N = 12$ ($N = 14$) as a result of symmetry

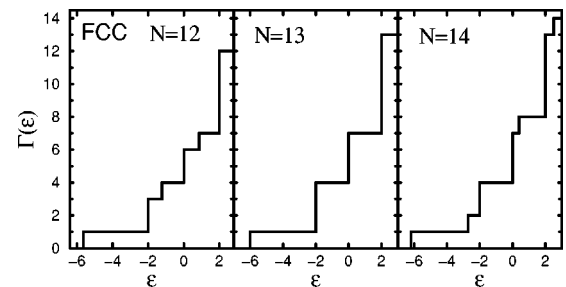


FIG. 6. Single-particle electronic structure of fcc clusters having $N = 12$ – 14 atoms. See caption of Fig. 3.

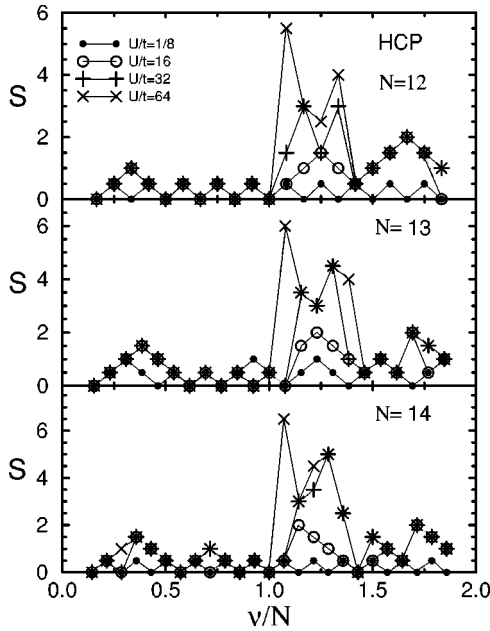


FIG. 7. Ground-state spin S of hexagonal-close-packed clusters having $N=12-14$ atoms as a function of band filling ν/N . The values of U/t are indicated.

lowering and lifting of degeneracies (compare Fig. 5 for $U/t=1/8$ and Fig. 6). Clusters with hcp structures show a qualitatively similar behavior. However, note that for small U/t the number of maxima ($S \geq 1$) is larger and the values of S are smaller than in fcc clusters, since the degeneracies of the SP levels are smaller (twofold at most). Removing or adding an atom lifts all SP degeneracies in hcp clusters (see Fig. 8 for $N=12$ and 14). Therefore, minimum S is obtained for all ν ($U/t=1/8$). Note that here the differences between the SP eigenvalues are very small (e.g., $\varepsilon_3 - \varepsilon_2 = 0.02t$ for $N=12$ and $\varepsilon_4 - \varepsilon_3 = 0.05t$ for $N=14$). As the Coulomb repulsion increases the details of the SP spectrum become less important and some of the differences between sizes and structures are removed. For example, all fcc clusters ($N=12-14$) have $S=3/2$ for $\nu=5$ and $S=3$ for $\nu_h=6$ if U/t is sufficiently large. Similar situations are found in hcp clusters (e.g., $S=1$ for $\nu=4$ and $S=2$ for $\nu_h=4$). However in other cases, such as the fcc cluster with $N=14$ and $\nu=4$ or $\nu_h=4$, the size and structural specificities remain even in the limit of $U/t \rightarrow \infty$.^{17,18}

A remarkable effect is observed in some fcc clusters having very small number of holes. For $\nu_h=2$ ($N=12$) and for $\nu_h=2$ and 3 ($N=13$) we find that two possible values of S

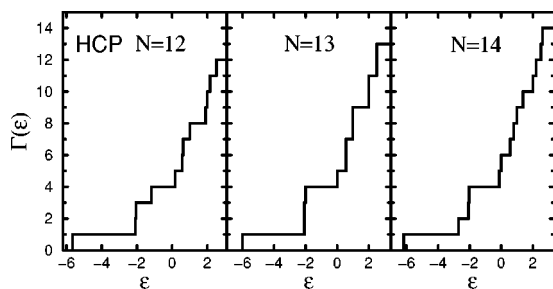


FIG. 8. Single-particle electronic structure of hcp clusters having $N=12-14$ atoms ($U=0$). See caption of Fig. 3.

are degenerate for all $U/t \geq 0$, at least within the accuracy of our calculations ($\sim 10^{-9}t$). This implies that for $\nu_h=2$ ($\nu_h=3$) a singlet (doublet) ground state is formed that has no empty-site configurations (no double-hole occupation on the same site) just as in the fully polarized triplet (quartet). Otherwise, the degeneracy would not hold for all U/t since $\partial E / \partial U = \sum_i \langle n_{i\uparrow} n_{i\downarrow} \rangle$. This particular behavior is most probably related to the exceptionally large degeneracy (five or six fold) of the highest antibonding state. We have not observed such an effect in any of the other studied clusters.

A simple interpretation of the magnetic properties in terms of the SP spectrum is no longer possible close to half-band filling ($0.5 < \nu/N < 1.5$). Here we observe a diversity of situations that defies simple generalizations. Below half-band filling low-spin states are usually obtained as in the icosahedral clusters. S is minimum for all U/t in spite of the presence of orbital degeneracies at $U=0$. See, for example, the results for the fcc 13-atom cluster with $\nu=10-13$. In other cases with SP orbital degeneracies, for instance, the fcc 14-atom cluster with $\nu=10$, $S=0$ for small U/t and a weakly magnetic ground state ($S=1$) is induced at larger U/t . A similar result is obtained in the hcp 14-atom cluster with $\nu=10$. Other clusters may show $S=1$ for small U/t and then lose their magnetic moment in the strongly correlated limit as a result of antiferromagnetism close to $\nu=N$. The hcp 13-atom cluster with $\nu=12$ is such an example. Above half-band filling ($1 < \nu/N < 1.5$) ferromagnetism develops more or less strongly with increasing Coulomb repulsion U/t . This trend is common to all compact (nonbipartite) structures. However, nonmonotonous behaviors as a function of U/t are also observed. For example, for fcc clusters with $N=13$ ($N=14$) and $\nu=17$ ($\nu=19$), S shows a minimum at intermediate values of U/t . In other cases ($N=14$, $\nu=16$, and fcc structure) S has a maximum as a function of U/t (see Fig. 5). This reflects subtle competitions between ferromagnetic and antiferromagnetic correlations.

Concerning the band-filling dependence of S in the strong ferromagnetic region ($1 < \nu/N < 1.5$) note that all considered fcc and hcp clusters present a maximum in S for $\nu/N=1.2-1.4$. Similar results are also obtained for icosahedral clusters (Sec. III A). Remarkably, the value of ν , which gives the maximum S at large U/t (e.g., $U/t=64$), is the same for all compact structures (icosahedral, fcc, or hcp). The details of the cluster geometry and, in particular, the presence or not of pentagonal loops, a characteristic of icosahedra, seem not to matter very much. However, triangular loops and the asymmetry of the SP spectrum are very important since bipartite structures like bcc clusters show a different behavior (see Sec. III C). The fact that the maximum S occurs in all sizes ($N=12-14$) at approximately the same ν/N suggests that in larger compact clusters ferromagnetism should also be particularly stable at these band fillings.

C. bcc clusters

The ground-state spin of bcc clusters is given in Fig. 9 as a function of band filling ν/N ($N=12-14$). First of all, let us recall that electron-hole symmetry implies $S(\nu) = S(2N - \nu)$, since the sign of the hopping integral t is irrelevant in bipartite structures.¹² In Fig. 9 results are shown below and above half-band filling mainly to facilitate the comparison

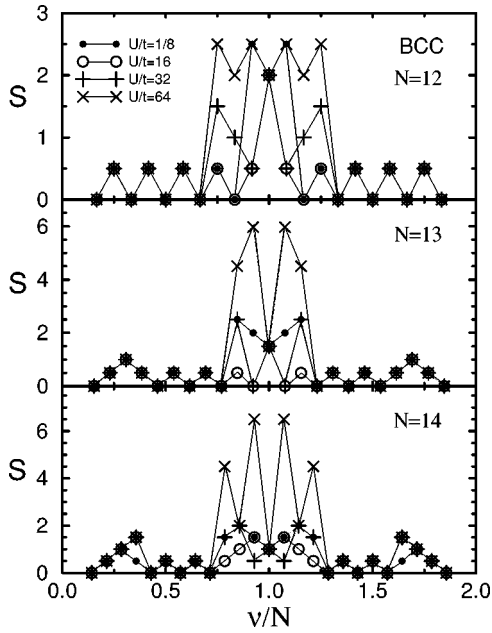


FIG. 9. Ground-state spin S of body-centered-cubic clusters having $N=12$ – 14 atoms as a function of band filling ν/N . The values of U/t are indicated.

with the previous compact structures. For low carrier concentrations (ν or $\nu_h < 0.5$) the band-filling dependence of S can be understood in terms of the SP spectra given in Fig. 10. For small U/t (e.g., $U/t=1/8$) S is minimal unless the highest occupied level is degenerate. In the latter case S corresponds to a full polarization of the electrons in the degenerate orbital (e.g., $S=1$ for $\nu=4$ and $N=13$ or 14). At small ν (or ν_h) S is generally independent of the value of the Coulomb repulsion. However, for some band fillings additional spin polarizations are induced by increasing U/t provided that the kinetic promotion energy (gap in the SP spectrum) is not too large. For instance, for $N=14$ and $\nu=5$ the gap in the SP spectrum is $\varepsilon_4 - \varepsilon_3 = 0.67t$ and $S=3/2$ for $U/t > 14.9$. Nevertheless, a reasonably small SP gap does not yield necessarily $S \geq 1$ even if $U/t \rightarrow \infty$. For example, in the $N=12$ bcc cluster, $\varepsilon_3 - \varepsilon_2 = 0.70t$ and still, one obtains $S=0$ for $\nu=4$ independently of U/t .¹⁹ Qualitatively similar behaviors are also found in nonbipartite structures (Secs. III A and III B).

As ν/N approaches half-band filling we first observe, for $0.5 < \nu/N < 0.75$, that the ground state has minimal S for all $U/t \geq 0$, even if orbital degeneracies would let $S \geq 1$ be expected. Consider, for example, $\nu=8$ for $N=12$, $\nu=8-10$

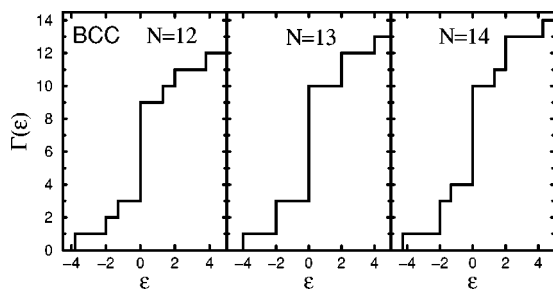


FIG. 10. Single-particle electronic structure of bcc clusters having $N=12$ – 14 atoms ($U=0$). See caption of Fig. 3.

for $N=13$, or $\nu=10$ for $N=14$, and compare Figs. 9 and 10. This demonstrates once more the importance of correlation effects in determining the relative stability of different magnetic solutions, particularly in the limit of $U/t \rightarrow \infty$.¹⁹ Note that in the Hartree-Fock approximation the energy of low-spin states is so overestimated that for large U/t a ferromagnetic-like state is always favored.

A variety of magnetic properties is found close to half-band filling ($0.75 < \nu/N < 1$). For $N=12$ sites with $\nu=9$ or 10 electrons, S increases with U/t starting from $S=0$ or $1/2$ and reaching eventually saturated values for sufficiently large U/t .¹⁹ In most cases, however, we obtain a nonvanishing magnetic moment already for small U/t , which first *decreases* with increasing U/t , before increasing again and surpassing the small- U/t magnetization at even larger U/t . Examples of this nonmonotonous behavior are found away from $\nu=N$ and include in particular Nagaoka's case: $\nu=11$ for $N=12$, $\nu=11$ and 12 for $N=13$, and $\nu=11$ – 13 for $N=14$. This can be regarded as the competition between weak ferromagnetism resulting from orbital degeneracies (small U/t), antiferromagnetic correlations that favor low-spin states and that dominate for intermediate U/t , and strong ferromagnetism at very large U where saturated or nearly saturated magnetic moments are obtained.

At half-band filling ($\nu=N$) we recover Lieb's theorem, which states that for all $U > 0$ the ground-state spin S of the half-filled Hubbard Hamiltonian on a bipartite lattice is $S = |N_A - N_B|/2$, where N_A and N_B are the number of sites belonging to the two sublattices A and B ($N = N_A + N_B$ even).²⁰ This result may be visualized as the spin of a perfect antiferromagnetic Néel state with sublattice magnetizations $N_A/2$ and $-N_B/2$, which need not cancel each other. Note that S is independent of U/t and that its value is not related to orbital degeneracies, for example, as one would obtain by applying Hund's rule to the SP spectra given in Fig. 10. As the cluster size grows the magnetic moment per atom of half-filled bcc clusters decreases with oscillations, since the differences between N_A and N_B can only originate at the outermost surface layers of the cluster [$(N_A - N_B)/N \rightarrow 0$ for $N \rightarrow \infty$]. Finally, we would like to point out that including next-NN hoppings in bcc clusters would result in asymmetric SP spectra and in antiferromagnetic frustrations. Therefore, one expects that in this case the magnetic behavior would tend to resemble qualitatively that of compact structures.

D. Structural stability and magnetic behavior

The ground-state energies are compared in order to determine the most stable of the considered structures (see Fig. 1). The results are summarized in the form of "phase" or structural diagrams as shown in Figs. 11–13. First of all, one observes that the three diagrams ($N=12$ – 14) reflect essentially the same physical behavior. Similar sequences of structures are obtained as the function of increasing band filling, for example, for small U/t the sequence icos-fcc-hcp-bcc and for $U/t \rightarrow \infty$ the sequence icos-hcp-fcc-bcc-icos-fcc-bcc. Remarkable similitudes are also found in the structural changes and magnetic transitions induced by varying the Coulomb repulsion. One concludes that the main trends in structure and magnetism as a function of ν/N and U/t are

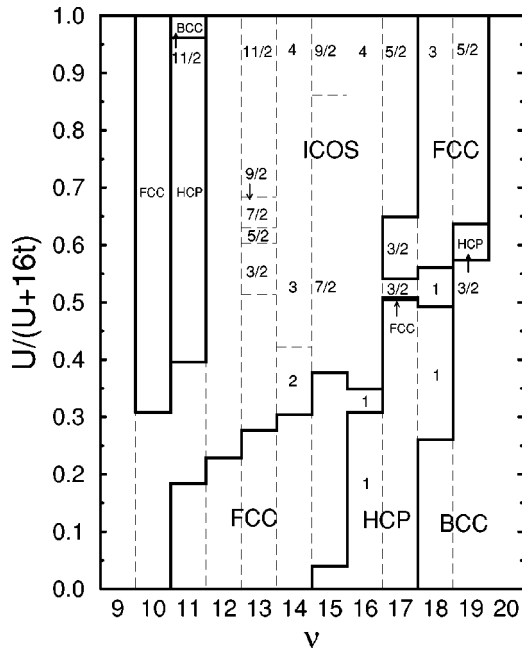


FIG. 11. Structural and magnetic diagram of Hubbard clusters having $N=12$ atoms as obtained by considering the icosahedral (icos), face-centered-cubic (fcc), hexagonal-close-packed (hcp), and body-centered-cubic (bcc) structures shown in Fig. 1. The most stable structure (among the considered ones) is given as a function of Coulomb repulsion U , hopping integral t , and number of electrons ν . The corresponding ground-state spin S is minimal ($S=0$ or $1/2$) unless explicitly indicated. Dashed lines separate regions having the same structure but different S . For $\nu \leq 9$ the icosahedron yields the lowest energy for all U/t , while for $\nu \geq 20$ the bcc structure is the most stable. For these band fillings, S is given in Figs. 2 and 9.

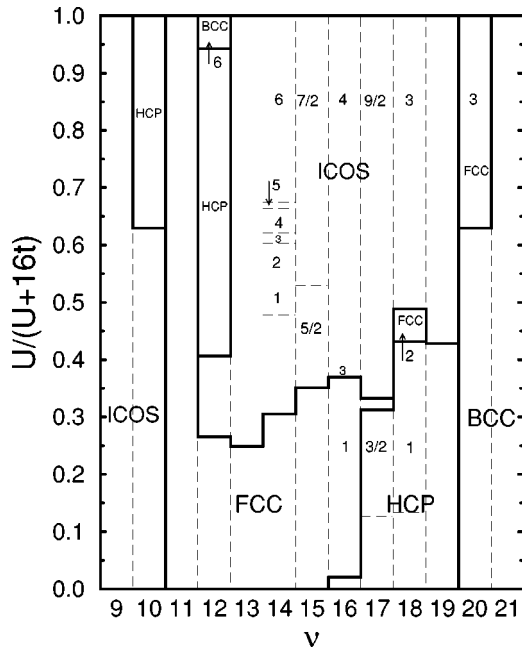


FIG. 12. Structural and magnetic diagram of Hubbard clusters having $N=13$ atoms as in Fig. 11. For $\nu \leq 9$ the icosahedron yields the lowest energy for all U/t , while for $\nu \geq 21$ the bcc structure is the most stable (see Figs. 2 and 9 for S at these band fillings).

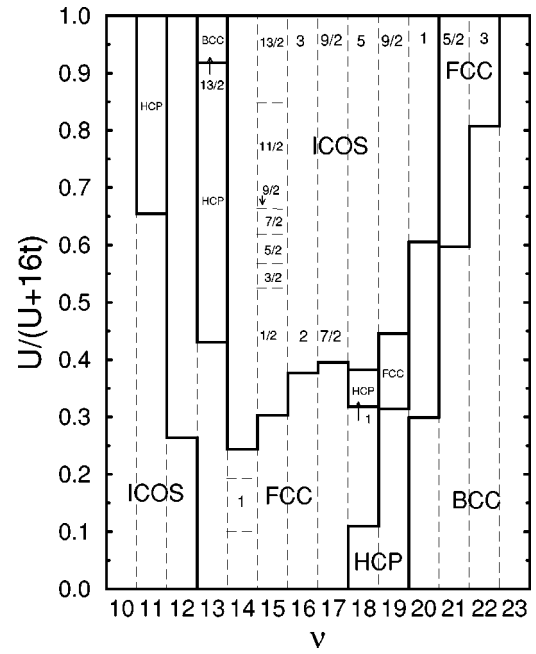


FIG. 13. Structural and magnetic diagram of Hubbard clusters having $N=14$ atoms as in Fig. 11. For $\nu \leq 10$ the icosahedron yields the lowest energy for all U/t , while for $\nu \geq 23$ the bcc structure is the most stable (see Figs. 2 and 9 for S at these band fillings).

not much affected by the symmetry changes caused by adding or removing an atom to perfect closed-shell surfaces ($N=13$).

For low electron or hole concentrations the lowest-energy structures (icosahedral for $\nu < 9-10$ and bcc for $\nu > 20-23$) are independent of U/t . The geometry that yields the lowest kinetic energy (uncorrelated limit) remains the most stable one irrespectively of the strength of the intra-atomic Coulomb interaction. The corresponding ground states have low spin. In some cases $S \geq 1$, which can be interpreted as the polarization of degenerate or quasidegenerate SP levels (see Secs. III A–III C). This indicates that for low carrier concentrations the effect of Coulomb interactions are considerably reduced by correlations, so that the magnetic and geometric structure of the clusters are dominated by the kinetic term. However, note that at least some of the magnetic states found for icosahedral or bcc clusters are probably irrelevant to the true ground-state phase diagram, since we have not fully optimized the cluster geometries. As already observed for $N \leq 8$,⁷ lower-symmetry structures may be found that are stabilized by removing SP degeneracies (Jahn-Teller effect) and that then often show minimal S . For small ν the most compact icosahedral structure yields the lowest energy, while for large ν the rather open bipartite bcc clusters are the most stable. This can be qualitatively understood in terms of the single-particle spectrum. In the first case (small ν) the largest stability corresponds to the largest bandwidth for bonding states ($\varepsilon_b \approx -\bar{z}t$) which is achieved by the most compact structure. In the second case (small ν_h) the largest stability is obtained for the largest bandwidth for antibonding (positive-energy) states, which corresponds to the bipartite structure. Qualitatively similar results are derived from exhaustive geometry optimizations for $N \leq 8$.⁷

Close to half-band filling ($10 \leq \nu \leq 22$) much more interesting electron-correlation effects on structure and magnetism are observed. For small U/t one finds fcc or hcp structures with very small, in most cases minimal, S . As U/t is increased a major change to the more compact icosahedral structure takes place [$U/(U+16t) > 0.3-0.4$]. In some cases this is preceded by transitions between fcc and hcp structures that reflect less important rearrangements of the positions of surface atoms. For $\nu=N$ we obtain $S=0$ or $1/2$ corresponding to frustrated antiferromagnets. In contrast, for $\nu > N$ the change from fcc or hcp to icosahedral structure is accompanied by an important increase of the total magnetic moment. This indicates that these structural changes are driven by ferromagnetism. Let us recall that high-spin states have a nearly completely filled majority band ($\nu > N$) and therefore the structural stability is dominated by the minority electrons. Since the minority band contains a small number of electrons, the most compact structures are favored. In fact, if the spin is saturated [$S=(2N-\nu)/2$ for $\nu > N$] the optimal structure for ν electrons coincides with the optimal structure for $2(\nu-N)$ electrons and $U=0$. This also explains qualitatively the transition from icosahedral to fcc structure by increasing ν observed at large U/t ($\nu > N$), which corresponds to a similar structural change at $\nu=10-11$ for small U/t ($N=13$). In addition note that ferromagnetism is much more frequent for $\nu > N$ than for $\nu \leq N$. Indeed, below half-band filling it is only observed for $\nu=N-1$ at very large U/t , where the bipartite bcc structure reaches a fully polarized Nagaoka state.

Before closing this section it is important to recall that the set of structures considered in this paper does not necessarily include the most stable one. In fact, previous studies of small clusters including geometry optimizations ($N \leq 8$) have already shown that the symmetry of the optimal structures is often reduced by distortions or rearrangements of bonds.⁷ Therefore, in order to explore the problem, we have considered a few additional structures for $N=13$ that are derived from the perfect fcc and icosahedral clusters by removing one or two surface bonds (i.e., by distorting the cluster surface). As in smaller clusters one observes that distortions may result in an energy lowering thereby improving the ground-state geometry. This usually occurs for intermediate values of U/t close to a major structural change (e.g., fcc to icosahedral at half-band filling). The calculated energy differences are in general very small (often less than a few percent of the total binding energy), which also suggests that similar structures may easily coexist at finite temperatures (small surface melting temperatures). Extending the geometry optimization studies up to $N=14$ would be very interesting in order to derive definitive conclusions on the interdependence of correlations, magnetism, and cluster structure in this size range.

IV. CONCLUSION

The magnetic properties of clusters having $N=12-14$ atoms have been studied in the framework of the Hubbard model by considering four different types of geometries (icosahedral, fcc, hcp, and bcc clusters). The ground states were calculated exactly for all band fillings and in the whole range of repulsive interactions ($U \geq 0$) by using a Lanczos numerical diagonalization method which involves no symmetry constraints.

For low electron or hole concentrations the ground-state spin S can be understood by applying Hund's first rule to the single-particle (SP) spectrum of the cluster as if it were a single structured atom. Thus, magnetic states ($S \geq 1$) are obtained when orbital degeneracies are present, or sometimes when the SP excitation energies are small if U/t is sufficiently large. Otherwise, the ground state has minimum spin multiplicity. Close to half-band filling a much more complex competition between low-spin and high-spin states is observed that defies simple generalizations. Remarkable features such as a decrease of S with increasing U/t or a non-monotonous dependence of S as a function of U/t are not uncommon. In particular, for $\nu/N=1.2-1.4$ we find that compact structures, which are the most stable geometries at these band fillings, show a strong tendency to ferromagnetism. In this case, ferromagnetism sets in for rather small values of U/t and in addition the ground-state spin S shows a maximum as a function of ν/N . In contrast, for $\nu \leq N$ low-spin states dominate even for very large U/t .

The trends on the relative stability between the different geometries are in qualitative agreement with previous calculations for $N \leq 8$.⁷ For small ν/N the most compact icosahedral structure yields the lowest energy, while for small ν_h/N ($\nu_h=2N-\nu$) the bipartite bcc structure is the most stable. For low carrier concentrations the lowest-energy structure is independent of U/t . In contrast, close to half-band filling several changes of structure are found, which are often accompanied by important changes in the magnetic behavior.

Multiband model extensions and systematic geometry optimizations are worth the development of further investigations in order to achieve a more realistic and detailed description of magnetic clusters. Rigorous calculations applying exact diagonalization methods to more complex Hamiltonians (e.g., including the full d -band degeneracy) not only have a fundamental interest on their own but would also serve as a basis for testing approximate methods applicable to larger clusters.

ACKNOWLEDGMENTS

Computer resources provided by IDRIS (CNRS, France) are gratefully acknowledged. One of the authors (F.L.U.) acknowledges support by CONACyT (Mexico).

¹W.A. de Heer, P. Milani, and A. Châtelain, Phys. Rev. Lett. **65**, 488 (1990); J.P. Bucher, D.C. Douglass, and L.A. Bloomfield, *ibid.* **66**, 3052 (1991); I.M.L. Billas, J.A. Becker, A. Châtelain, and W.A. de Heer, *ibid.* **71**, 4067 (1993); A.J. Cox, J.G. Loudereback, and L.A. Bloomfield, *ibid.* **71**, 923 (1993); A.J. Cox,

J.G. Loudereback, S.E. Apsel, and L.A. Bloomfield, Phys. Rev. B **49**, 12 295 (1994); I.M.L. Billas, A. Châtelain, and W.A. de Heer, Science **265**, 1682 (1994); S.E. Apsel, J.W. Emmert, J. Deng, and L.A. Bloomfield, Phys. Rev. Lett. **76**, 1441 (1996).
²D.R. Salahub and R.P. Messmer, Surf. Sci. **106**, 415 (1981); C.Y.

- Yang, K.H. Johnson, D.R. Salahub, J. Kaspar, and R.P. Messmer, *Phys. Rev. B* **24**, 5673 (1981); K. Lee, J. Callaway, and S. Dhar, *ibid.* **30**, 1724 (1985); K. Lee, J. Callaway, K. Wong, R. Tang, and A. Ziegler, *ibid.* **31**, 1796 (1985); K. Lee and J. Callaway, *ibid.* **48**, 15 358 (1993); G.M. Pastor, J. Dorantes-Dávila, and K.H. Bennemann, *Physica B* **149**, 22 (1988); *Phys. Rev. B* **40**, 7642 (1989); J. Dorantes-Dávila, H. Dreyssé, and G.M. Pastor, *ibid.* **46**, 10 432 (1992); B.I. Dunlap, *Z. Phys. D* **19**, 255 (1991); J.L. Chen, C.S. Wang, K.A. Jackson, and M.R. Pederson, *Phys. Rev. B* **44**, 6558 (1991); M. Castro and D.R. Salahub, *ibid.* **49**, 11 842 (1994); P. Ballone and R.O. Jones, *Chem. Phys. Lett.* **233**, 632 (1995); B.V. Reddy, S.N. Khanna, and B.I. Dunlap, *Phys. Rev. Lett.* **70**, 3323 (1993); B. Piveteau, M-C. Desjonquères, A.M. Olés, and D. Spanjaard, *Phys. Rev. B* **53**, 9251 (1996); J. Dorantes-Dávila, P. Villaseñor-González, H. Dreyssé, and G.M. Pastor, *ibid.* **55**, 15 084 (1997).
- ³J. Hubbard, *Proc. R. Soc. London, Ser. A* **276**, 238 (1963); **281**, 401 (1964); J. Kanamori, *Prog. Theor. Phys.* **30**, 275 (1963); M.C. Gutzwiller, *Phys. Rev. Lett.* **10**, 159 (1963).
- ⁴L.M. Falicov and R.H. Victora, *Phys. Rev. B* **30**, 1695 (1984).
- ⁵Y. Ishii and S. Sugano, *J. Phys. Soc. Jpn.* **53**, 3895 (1984).
- ⁶J. Callaway, D.P. Chen, and R. Tang, *Z. Phys. D* **3**, 91 (1986); *Phys. Rev. B* **35**, 3705 (1987).
- ⁷G.M. Pastor, R. Hirsch and B. Mühlischlegel, *Phys. Rev. Lett.* **72**, 3879 (1994); *Phys. Rev. B* **53**, 10 382 (1996).
- ⁸Y. Wang, T.F. George, D.M. Lindsay and A.C. Beri, *J. Chem. Phys.* **86**, 3493 (1987).
- ⁹In Ref. 7 exact diagonalization methods have been applied to study the stability of saturated ferromagnetism in 13-atom clusters. The single-spin-flip energy $\Delta\varepsilon_{sf}$ was determined in the limit of infinite U/t and the band-filling dependence of $\Delta\varepsilon_{sf}$ was correlated to electronic shell closings in the single-particle spectrum.
- ¹⁰C. Lanczos, *J. Res. Natl. Bur. Stand.* **45**, 255 (1950); B.N. Parlett, *The Symmetric Eigenvalue Problem* (Prentice-Hall, Englewood Cliffs, NJ, 1980); J.K. Collum and R.A. Willoughby, *Lanczos Algorithms for Large Symmetric Eigenvalue Computations* (Birkhauser, Boston, 1985), Vol. I.
- ¹¹A structure is called *bipartite* if two distinct subsets of lattice sites A and B can be defined such that every lattice site belongs either to A or to B and that there is no pair of NN's belonging to the same subset. All NN bonds (or hoppings) connect a site in A with a site in B .
- ¹²The electron-hole transformation $h_{i\sigma}^\dagger = c_{i\bar{\sigma}}$ leaves the Hamiltonian formally unchanged, except for an additive constant and a change of sign in the hopping integrals, which amounts to an inversion of the SP spectrum ($\varepsilon_k \rightarrow -\varepsilon_k$).
- ¹³We have performed calculations on icosahedral clusters ($N = 12-14$) for $U/t = +\infty$ by projecting out double electron (hole) occupations for $\nu < N$ ($\nu > N$). The only differences between $U/t = \infty$ and $U/t = 64$ are the following. $N = 12$: $S = 1, 4$, and $9/2$ for $\nu = 10, 14$, and 15 , respectively. $N = 13$: $S = 1$ for $\nu = 10$. $N = 14$: $S = 13/2$ for $\nu = 15$. In particular for $\nu/N < 0.5$ and $\nu/N > 1.5$, the results for $U/t = 64$ and $U/t = \infty$ coincide.
- ¹⁴For $N = \nu = 13$ and $4.6 \leq U/t \leq 20$ we find vanishing NN spin correlations that can be interpreted as a resonant-valence-bond-like state (see Ref. 15). A detailed discussion of the U/t dependence of spin-correlation functions close to half-band filling is beyond the scope of this paper and will be reported elsewhere.
- ¹⁵J. Callaway, *Phys. Rev. B* **35**, 8723 (1987).
- ¹⁶Y. Nagaoka, *Solid State Commun.* **3**, 409 (1965); D.J. Thouless, *Proc. Phys. Soc. London* **86**, 893 (1965); Y. Nagaoka, *Phys. Rev.* **147**, 392 (1966); H. Tasaki, *Phys. Rev. B* **40**, 9192 (1989).
- ¹⁷For $U/t = \infty$ the following S are obtained in fcc clusters. $N = 12$: $S = 1$ for $\nu = 6$ and $S = 4$ for $\nu = 14$. $N = 13$: $S = 9/2$ for $\nu = 15$ and $S = 4$ for $\nu = 16$. $N = 14$: $S = 6, 5/2$, and 2 for $\nu = 16, 19$, and 24 , respectively. Otherwise, the results for $U/t = \infty$ coincide with those for $U/t = 64$ reported in Fig. 5.
- ¹⁸For $U/t = \infty$ the S of hcp clusters are the following. $N = 12$: $S = 3/2, 4, 7/2$, and $7/2$ for $\nu = 5, 14, 15$, and 17 , respectively. $N = 13$: $S = 9/2$ for $\nu = 15$ and $S = 4$ for $\nu = 16$. $N = 14$: $S = 6, 7/2$, and 2 for $\nu = 16, 19$, and 20 , respectively. Otherwise, $S(U/t = \infty)$ coincides with $S(U/t = 64)$.
- ¹⁹For $U/t = \infty$ the S of bcc clusters are the same as for $U/t = 64$ except in the following cases. $N = 12$: $S = 5$ for $\nu = 10$ and $\nu = 14$, $S = 11/2$ for $\nu = 11$ and $\nu = 13$. $N = 13$: $S = 7/2$ for $\nu = 11$ and $\nu = 15$. $N = 14$: $S = 3$ for $\nu = 12$ and $\nu = 16$.
- ²⁰E.H. Lieb, *Phys. Rev. Lett.* **62**, 1201 (1989).